Reply to "Comment on 'Coexistence of ferromagnetism and superconductivity in Sn nanoparticles' "

Wen-Hsien Li* and Chun-Ming Wu
Department of Physics, National Central University, Jhongli 32001, Taiwan
(Received 19 October 2009; revised manuscript received 17 May 2010; published 22 July 2010)

In this Reply we show that the thermal characteristic of μ_p increases with increasing temperature remains when size distribution of the nanoparticle assembly has been accounted for. In addition, the antiferromagneticlike or ferrimagneticlike spin configuration is also required to understand the two-component hysteresis observed in the $M(H_a)$ curves. The appearance of hysteresis in the low H_a regime [Fig. 4 of W.-H. Li, C.-W. Wang, C.-Y. Li, C. K. Hsu, C. C. Yang, and C.-M. Wu, Phys. Rev. B **77**, 094508 (2008)] indicates the existence of a net spontaneous moment in the nanoparticle, whereas the enlarged hysteresis at the high H_a regime can be the results of the occurrence of spin reorientation of the core and surface macromoments triggered by the applied magnetic field.

DOI: 10.1103/PhysRevB.82.016504 PACS number(s): 74.81.Bd, 73.63.Bd, 74.62.Yb, 81.07.Wx

In his Comment the author claims that the linear increase in the average particle moment μ_p with increasing temperature observed in the 14 nm Sn nanoparticle (NP) assembly, shown in Fig. 5 of Ref. 1, cannot be explained using the mechanism of thermoinduced magnetization,[2] rather it should be resulting from ignoring the size distribution of the nanoparticle assembly.[3] The author argues that the thermoinduced mechanism is not appropriate due to the lack of antiparallel sublattice spins in Sn nanoparticles and the temperature behavior of saturation magnetization $M_S(T)$ does not scale with that of $N\mu_p(T)$, where N is the number of Sn nanoparticles per gram.

Although the size distribution of the NP assembly can affect the apparent thermal behavior of μ_p but the significance of the effect depends strongly on the size dispersion of the assembly.[3] The size distribution of our NP assembly can be described by a Gaussian function, with a center at 13.8 nm and a half width of 2.8 nm (Fig. 2 of Ref. 1). In accounting for the contributions from every size of the particles in the assembly, the magnetization takes the form of

$$M(H_a,T) = C_0 \sum_i n_i \mu_{pi} L\left(\frac{\mu_{pi} H_a}{k_B T}\right) + \chi_D H_a,$$

where i denotes the contributions from a particular size of the particles, n_i indicates the number of particles per gram of the corresponding size, C_0 is the conversion constant between the units of electromagnetic unit and Bohr magneton μ_B, and χ_D is the Lentz diamagnetic susceptibility. Unfortunately, the dependency of particle moment on the particle size of Sn nanoparticles is currently not available. The open circles in Fig. 1 mark the $\mu_p(T)$ obtained assuming a lognormal moment distribution with respect to the particle diameter

$$\mu_{pi}(d_i) = \frac{\mu_0}{w\sqrt{2\pi}} \exp\left\{-\frac{(\ln d_i - \ln d_m)^2}{2w^2}\right\},$$

where μ_0, w, and d_m represent the magnitude, the width, and the mode of the moment distribution, respectively. All the particle sizes shown in Fig. 2 of Ref. 1 are accounted for in the fits, with μ_0, w, d_m, n_i, and χ_D being the fitting parameters. μ_p of the 14 nm Sn particles can then be extracted from the moment distribution parameters μ_0, w, and d_m obtained from the fits.

Figure 1 clearly reveals that the thermal increase rate of the μ_p obtained when size distribution has been accounted for is considerably smaller than those upon assuming a monodispersed particle assembly. Nevertheless, the thermal characteristic of μ_p increases with increasing temperature remains. It is then *not* the size dispersion that governs the thermal behavior of μ_p shown in Fig. 1. This thermal profile of μ_p increases with increasing temperature can be understood by thermal-induced magnetization,[4] which requires an antiferromagnetic or a ferrimagnetic configuration. The dash curve in Fig. 1 indicates the fit of the observed $\mu_p(T)$ to the expression[4] of antiferromagnetic thermoinduced spin-wave excitations listed in the plot to give $\mu_{p0} \equiv \mu_p(T=0) = 82.5\ \mu_B$, which indicates the mean spontaneous particle moment without contribution from thermal excitations. We note that the fits to the $M(H_a)$ curves are slightly better when size distribution is incorporated. No significant difference in the thermal behavior of μ_p, but a slightly larger thermal increase rate, is obtained when assuming a Gaussian or a Lorentzian moment distribution.

The antiferromagneticlike or ferrimagneticlike criterion is also required to understand the significantly larger hystereses appear in the high H_a regime of the $M(H_a)$ curve shown in Fig. 2. These hystereses appear when H_a is stronger than ~ 0.3 T but not weaker, showing that a relatively large critical H_a is indeed needed in triggering them. In addition, the opening in M becomes smaller when H_a excesses 2.5 T. Both behaviors are characteristics of the magnetic moments being reoriented by an external magnetic field. They can be understood by consider the magnetic energy associated with the core moment $\mathbf{m_1}$ and surface moment $\mathbf{m_2}$, as illustrated in the inset to Fig. 2, under a field increasing followed by a field-decreasing loop. The magnetic energy of the particle, when it is subjected to an H_a, takes the form of

$$E_m = -m_1 H_a \cos\theta_1 - m_2 H_a \cos\theta_2 + k_1 \sin^2(\theta_1 - \varphi_1) + k_2 \sin^2(\theta_2 - \varphi_2),$$

where θ_1 and θ_2 indicate the deviations of $\mathbf{m_1}$ and $\mathbf{m_2}$ from

 ©2010 The American Physical Society

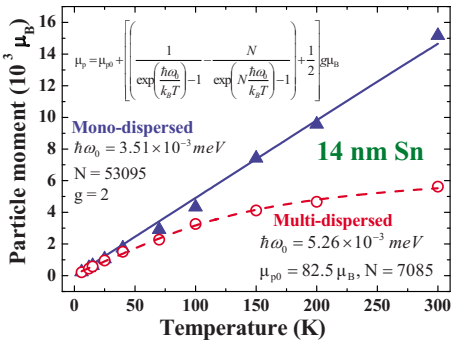

FIG. 1. (Color online) Temperature dependencies of μ_p obtained when the size distribution is incorporated (open circles) together with that when assuming a monodispersed particle assembly (solid triangles, Fig. 5 of Ref. 1). Both $\mu_p(T)$ curves reveal that μ_p increases with increasing temperature. The solid and dashed curves indicate the results of fits to the expression listed in the plot.

the field direction, φ_1 and φ_2 indicate the deviations of the corresponding easy axes from the field direction, k_1 and k_2 are the corresponding anisotropy strengths. The magnetization can readily be calculated by evaluating $M(H_a) = m_1 \cos\theta_{1m} + m_2 \cos\theta_{2m}$, where θ_{1m} and θ_{2m} are the θ_1 and θ_2, respectively, that minimize E_m at each H_a. Figure 3 displays the magnetization loop at 50 K when the Lentz diamagnetic component has been subtracted for simplicity. The solid curve in Fig. 3 indicates the calculated $M(H_a)$ loop thus obtained. Taking $\mu_{p0}=82.5\ \mu_B$ and $m_2/m_1=1.045$ give $m_1 = 1833\ \mu_B$ and $m_2=1916\ \mu_B$, when assuming m_1 and m_2 are exactly antiparallel at zero temperature. The $m_2=1916\ \mu_B$ corresponds to an uncompensated spin of $1916/13\,280 = 0.15$ electrons/atom on the surface shell, when assuming it consists of only one layer of atoms.

The saturation magnetization of the assembly at a temperature T is then obtained according to $M_S(T)=C_0\Sigma_i n_i\mu_{pi}$. Their temperature dependence is plotted in Fig. 4(a). No significant reduction but a small bump at 50 K is seen in M_S from 6 to 300 K. It behaves differently from the thermal behavior observed for μ_p (Fig. 1). This discrepancy between the thermal profiles of M_S and μ_p is not completely understood at the present time but the thermal reduction in the numbers of magnetic particles can play a role. We note that μ_p is determined mainly by the slope of the $M(H_a)$ curve in the low-field regime, whereas M_S reflects primary the maximum value of M that appears in the high-field regime. Fits *cannot* converge if setting M_S proportional to μ_p but need two independent parameters to describe particle moment μ_{pi} and saturation magnetization $n_i\mu_{pi}$ for the observed $M(H_a)$ curves. It is the decrease in n_i with increasing temperature that counter balance the increase in μ_{pi} with increasing temperature, such that M_S and μ_p behave differently in a thermal process. These n_i then indicate the numbers of magnetic particles, which do not remain at constant values but appear to decrease with increasing temperature from the fits. Figure 4(b) shows the temperature dependence of Lentz diamagnetic susceptibility χ_D. It increases by a factor of 2.25, with a bump at 50 K, from 6 to 300 K. The origins that give rise

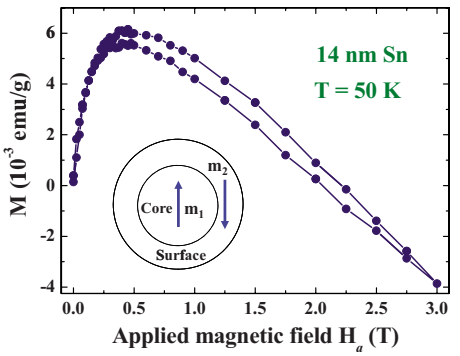

FIG. 2. (Color online) Magnetization loops of the 14 nm Sn particles taken at 50 K, revealing the appearance of magnetic hysteresis in the high magnetic field regime. The inset shows the schematic illustration of the core macromoment $\mathbf{m_1}$ and the surface macromoment $\mathbf{m_2}$ in Sn nanoparticles.

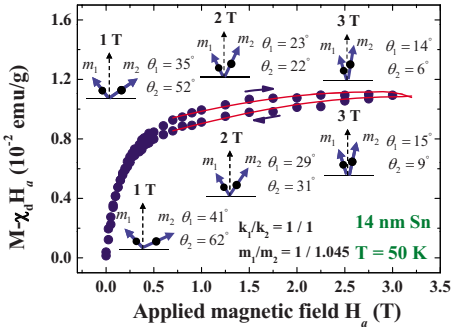

FIG. 3. (Color online) Variations in M-$\chi_D H_a$ with applied magnetic field of the 14 nm Sn particle assembly, taken at 50 K along a field increasing followed by a field-decreasing loop. The solid curve indicates the magnetization curve calculated using the parameters listed in the plot. An $m_2/m_1=1.045$ is obtained.

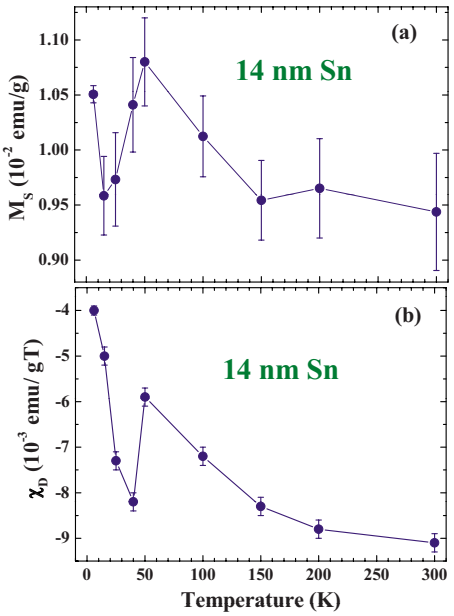

FIG. 4. (Color online) Temperature dependencies of (a) the saturation magnetization and (b) the Lentz diamagnetic susceptibility of the 14 nm Sn particle assembly.

to the bumps at 50 K in the $M_S(T)$ and $\chi_D(T)$ curves need further investigation. Although χ_D can affect the fitted values for M_S but it will not significantly alter the thermal profile of M_S.

The development of magnetism in metallic nanoparticles is nowadays attributed to the appearance of uncompensated spins originated from the spreading of Fermi holes[5] and/or from the transferring of charges[6] between the interior and the surface regions of the particles. Unfortunately, the details of the spin arrangements in metallic nanoparticles remain covered. It is very unlikely that every Sn ion in a 14 nm particle contribute an aligned spin to form a conventional magnetic configuration. Apparently, the atoms in a nanoparticle can be distinguished into the core and the surface atoms since the crystalline environments for the former and for the latter are apparently different. The spreading of Fermi holes and/or the transferring of charges between the core and surface atoms will result in a different charge and spin distribution for the two regions. Different magnetic characteristics for the core and for the surface regions can then be anticipated. As we have pointed out in Ref. 1, the magnetic moment of a Sn nanoparticle is taken as from a macrospin. This macrospin of a Sn nanoparticle may be viewed as consisting of a core macromoment $\mathbf{m_1}$ and a surface macromoment $\mathbf{m_2}$, as illustrated in the inset to Fig. 2. Each of which indicates the net moment in the corresponding region. Our observation of μ_p increases as the temperature is increased (Fig. 1) cannot be understood when taking all the uncompensated moments are pointed in the same direction, i.e., a ferromagneticlike nanoparticle but need at least some of them point in the opposite direction, i.e., a ferrimagneticlike nanoparticle. This criterion is also needed in understanding the enlarged magnetic hystereses appear in the high H_a regime shown in Fig. 3. The two-component hysteresis observed in the $M(H_a)$ curves of the present 14 nm Sn particle assembly can then be understood as the following: the appearance of hysteresis in the low H_a regime (Fig. 4 of Ref. 1) indicates the existence of a net spontaneous moment in the nanoparticle, whereas the enlarged hysteresis at the high H_a can be the results of the occurrence of spin reorientation of $\mathbf{m_1}$ and/or $\mathbf{m_2}$ triggered by H_a. This spin reorientation scenario has also been suggested in understanding the hysteresis loops observed in Ag-C core-shell nanocomposites.[7] The two-component hysteresis observed in the $M(H_a)$ curves *cannot* be anticipated in ferromagneticlike particles but require again a ferrimagneticlike configuration, i.e., $\mathbf{m_1}$ and $\mathbf{m_2}$ points in the opposite directions but result in a net macromoment for the nanoparticle, as has been suggested for Au nanoparticles.[8] The thermal reductions in the numbers of the magnetic particles result in a different thermal profiles for μ_p and for M_S.

*Corresponding author; whli@phy.ncu.edu.tw

[1] W.-H. Li, C.-W. Wang, C.-Y. Li, C. K. Hsu, C. C. Yang, and C.-M. Wu, Phys. Rev. B **77**, 094508 (2008).
[2] S. Mørup and C. Frandsen, Phys. Rev. Lett. **92**, 217201 (2004).
[3] N. J. O. Silva, L. D. Carlos, and V. S. Amaral, Phys. Rev. Lett. **94**, 039707 (2005).
[4] S. Mørup and B. Rosendahl Hansen, Phys. Rev. B **72**, 024418 (2005).
[5] H. J. Juretschke, Phys. Rev. **92**, 1140 (1953); M. K. Harbola and V. Sahni, Phys. Rev. B **37**, 745 (1988).
[6] C. M. Chang and M. Y. Chou, Phys. Rev. Lett. **93**, 133401 (2004); M. Pereiro and D. Baldomir, Phys. Rev. A **72**, 045201 (2005).
[7] R. Caudillo, X. Gao, R. Escudero, M. Jose-Yacaman, and J. B. Goodenough, Phys. Rev. B **74**, 214418 (2006).
[8] C.-M. Wu, C.-Y. Li, Y.-T. Kuo, C.-W. Wang, S.-Y. Wu, and W.-H. Li, J. Nanopart. Res. **12**, 177 (2010).